REPORT DOCUMENTATION PAGE

Form Approved
OMB NO. 0704-0188

1. AGENCY USE ONLY (Leave Blank)	2. REPORT DATE December 07, 2004	3. REPORT TYPE AND DATES COVERED Final Progress Report 01 NOV 00 - 31 oct 04

4. TITLE AND SUBTITLE
CHEMICAL KINETICS AND AERODYNAMICS OF IGNITION

5. FUNDING NUMBERS
DAAD19-01-1-0004

6. AUTHOR(S)
Chung K. Law

7. PERFORMING ORGANIZATION NAME(S) AND ADDRESS(ES)
Department of Mechanical and Aerospace Engineering
Princeton University, Princeton, NJ 08544

8. PERFORMING ORGANIZATION REPORT NUMBER

9. SPONSORING / MONITORING AGENCY NAME(S) AND ADDRESS(ES)
U. S. Army Research Office
P.O. Box 12211
Research Triangle Park, NC 27709-2211

10. SPONSORING / MONITORING AGENCY REPORT NUMBER

41267.7 - EG

11. SUPPLEMENTARY NOTES

12 a. DISTRIBUTION / AVAILABILITY STATEMENT
Approved for public release; distribution unlimited.

12 b. DISTRIBUTION CODE

13. ABSTRACT (Maximum 200 words)

The present program aimed to study ignition in nonhomogeneous systems that are of relevance to practical combustion devices. The investigation was conducted in both laminar and turbulent environments, and involved experimental, computational, and analytical components.

For turbulent ignition, four specific projects were undertaking, namely: (1)Characterization of non-reacting turbulent flow fields in counterflow; (2)turbulent non-premixed ignition experiments; (3)modeling study of turbulent nonpremixed ignition; (4)computational simulation of the ignition of an nonpremixed hydrogen/air mixing layer with an embedded vortex.

In parallel, three projects in laminar premixed and nonpremixed counterflow were explored, especially focusing on the chemical kinetics aspects and the coupling with transport, namely: (1) Premixed hydrogen/air and propane/air ignition; (2) experimental determination and computational calculation of the counterflow ignition temperatures and laminar flame speeds of several C2-C3 hydrocarbons; (3) experimental determination and computational calculation of the ignition temperatures of nonpremixed counterflow dimethyl ether (DME) versus air.

14. SUBJECT TERMS
Chemical kinetics, ignition, laminar counterflow ignition, turbulent and vortex ignition, hydrogen, dimethyl ether, C2-C3 hydrocarbons

15. NUMBER OF PAGES
17

16. PRICE CODE

17. SECURITY CLASSIFICATION OR REPORT UNCLASSIFIED	18. SECURITY CLASSIFICATION ON THIS PAGE UNCLASSIFIED	19. SECURITY CLASSIFICATION OF ABSTRACT UNCLASSIFIED	20. LIMITATION OF ABSTRACT UL

Enclosure 1

Final Progress Report

(September 1, 2000 to August 31, 2004)

CHEMICAL KINETICS AND AERODYNAMICS OF IGNITION

(DAAD19-01-1-0004)

Submitted By:

Chung K. Law

Department of Mechanical and Aerospace Engineering

Princeton University, Princeton, NJ 08544

Phone: 609-258-5271

Fax: 609-258-6233

E-Mail: cklaw@princeton.edu

For Consideration By:

Dr. David Mann

Army Research Office

20050201 039

1

Table of Contents

CHEMCIAL KINETICS AND AERODYNAMICS OF IGNITION

(DAAD19-01-1-0004)

Chung K. Law
Department of Mechanical and Aerospace Engineering
Princeton University, Princeton, NJ 08544
609-258-5271 (Voice); 609-258-6233 (Fax); cklaw@princeton.edu

Statement of Problem

The present program aimed to study ignition in nonhomogeneous systems that are of relevance to practical combustion devices. The investigation was conducted in both laminar and turbulent environments, and involved experimental, computational, and analytical components.

For turbulent ignition, four specific projects were undertaking, namely: (1) Characterization of non-reacting turbulent flow fields in counterflow, in which the velocity moment along the counterflow axis, mean and fluctuating velocity profiles, and turbulent power spectrum were measured for a wide range of pressures, bulk strain rates, perforated plate configurations, and air temperatures; (2) turbulent non-premixed ignition experiments, for which ignition temperatures were determined for hydrogen for a range of turbulent flows, fuel concentrations, and pressures. It was observed that optimal conditions for ignition exist in weakly turbulent flows where the ignition temperature is lower than either laminar or strongly turbulent flows at the same pressure; (3) modeling study of turbulent nonpremixed ignition, which was conducted by using Monte Carlo techniques to solve a joint scalar PDF equation to assist the understanding of our turbulent ignition experimental results; (4) computational simulation of the ignition of a nonpremixed hydrogen/air mixing layer with an embedded vortex with detail chemistry, showing that the scalar dissipation rate is a crucial controlling factor for ignition, causing a nonmonotonic dependence of ignition delay on various vortex parameters.

In parallel, three projects in laminar premixed and nonpremixed counterflows were explored, especially focusing on the chemical kinetics aspects and the coupling with transport, namely: (1) Premixed hydrogen/air and propane/air ignition, showing that diffusion can modify the local ignition kernel conditions to be different with the boundary conditions, and as a consequence the hydrogen premixed ignition exhibits five limits in the pressure-temperature diagram; (2) experimental determination and computational calculation of the counterflow ignition temperatures and laminar flame speeds of several C_2-C_3 hydrocarbons, showing deficiencies in literature mechanisms; (3) experimental determination and computational calculation of the ignition temperatures of nonpremixed counterflow dimethyl ether (DME) versus air, leading to the validation of a recent mechanism that showed very close agreement with the experimental data.

Summary of Results

1. Effects of Turbulence on Ignition

1.1 Characterization of non-reacting turbulent flow fields

High fidelity experimental data for turbulent non-reacting counterflows are necessary to interpret turbulent non-premixed ignition experiments and to develop and evaluate numerical models for turbulent ignition. It is particularly important to have measurements of counterflows where one jet has a significantly different density than the other, as such data is not available in the literature. Counterflowing jets of heated air and cold nitrogen were investigated using a two-component laser Doppler anemometry system to measure velocity moments, spectra, and autocorrelations throughout the flow field. Operating conditions spanned a range of pressures, bulk strain rates, perforated plate configurations, and air temperatures. In addition to measuring velocity moments along the counterflow axis, mean and fluctuating velocity profiles were made in the radial direction at each nozzle exit. These profiles are important for establishing boundary conditions in turbulent flow models. The radial velocity gradients are needed in quasi-one dimensional turbulence models and the profiles themselves are needed for higher dimensional Reynolds stress models and Large Eddy Simulations.

Autocorrelation measurements at the burner exits were used with Taylor's hypothesis to estimate the flow's integral length scale. The length scales were about 70% of the perforated plate hole diameters, in agreement with theory and other experiments. The length scale is important for modeling efforts since it can be used to estimate the turbulent dissipation rate.

Turbulent power spectra were determined at the burner exits to further characterize the turbulence for a given perforated plate configuration. For example, due to the difficulties associated with generating turbulence in a strongly heated flow, some experiments have been conducted with only one perforated plate, located in the cold flow. The use of this configuration was justified by the observation that the turbulent fluctuations resemble those in a turbulent counterflow that has perforated plates in both nozzles. However, a comparison of the power spectra measured at the hot side of the burner shows that there is a significant difference between the two cases. The spectrum of the case without a second perforated plate is suggestive of very young, undeveloped turbulence, indicating that it is important to have a perforated plate in both sides of the burner when studying turbulence.

1.2 Turbulent non-premixed ignition experiments

Our previous studies on turbulent nonpremixed ignition were performed in the counterflow configuration, with turbulence generated by a perforated plate in the fuel side of the flow as was done by other studies involving counterflow turbulent combustion. For the hydrogen/air system, it was found that the turbulence intensity of the flow did not have an appreciable effect on the ignition temperature. These results were understood to reflect the facts that, in laminar flows, hydrogen ignition is relatively insensitive to strain rate variations under second-limit conditions such as those present at atmospheric pressure, and that the role of turbulence in the flows studied was felt

4

primarily in the form of a turbulent strain rate. However, since in these experiments turbulence was generated only on the fuel side, while the ignition kernel was located on the oxidizer side, it is not certain how representative the results are of real turbulent conditions. Thus a major objective of the present investigation was to study ignition with turbulence generated on both sides of the flow by using two perforated plates. Results that are qualitatively different from the previous work were observed and are reported in the following.

Ignition temperatures were determined for hydrogen for a range of turbulent flows, fuel concentrations, and pressures. In the pseudo-turbulent configuration of one perforated plate, the flows are characterized by a narrow range of large scale, low frequency fluctuations that produce a quasi-steady response. With perforated plates on both sides of the flow, the lowest turbulence intensity investigated significantly reduced ignition temperatures at atmospheric pressure relative to laminar values as shown in Fig. 1. Subsequent increases in turbulence intensity caused the ignition temperatures to rise and the dependence on the bulk strain rate to weaken. These results indicate that optimal conditions for ignition exist in weakly turbulent flows and these temperatures are notably lower than can be obtained at the same pressure in laminar flows. Compared to pseudo-turbulent flows, fully turbulent flows have a wider range of eddy sizes that extend to much smaller scales, thereby affecting the structure of the ignition kernel and the ignition behavior.

The effects of varying the fuel concentration in turbulent flows were found to be qualitatively similar to those in laminar flows; ignition is relatively insensitive to fuel concentration at high fuel concentrations and becomes increasingly more sensitive at lower concentrations. The relative order of the ignition temperatures between different flows was the same for all fuel concentrations.

The effect of pressure on ignition is of particular interest due to the prominently nonlinear nature of the hydrogen oxidation kinetics as exemplified by the p-T explosion limits. Further experiments were conducted at three turbulence intensities and pseudo-turbulent flows at pressures ranging from 0.6atm to 8atm and a fuel concentration fixed at 20%. Results are shown in Fig. 2 for two different pressure-weighted strain rate ranges, with laminar calculations and crossover temperatures included for comparison. The increase in ignition temperature associated with increasing turbulence intensity, noted above for one atmosphere, is seen to hold for all pressures studied. Furthermore, the large decrease in ignition temperature from laminar ignition to the lowest turbulence intensity is found to hold for pressures throughout the second ignition limit. However, at higher pressures, the laminar ignition temperature increases more slowly as the transition occurs between the second and the third ignition limits so that at a fixed pressure the turbulent ignition temperature becomes higher than the laminar calculation. At the lower bulk strain rates of Fig. 2a, the turbulent ignition response seems to undergo a transition to the third limit where the ignition temperature decreases with increasing pressure, although this transition occurs at 6atm. in the turbulent flows rather than at 5atm. in a laminar flow with a similar strain rate. The data at the higher bulk strain rates in Fig. 2b do show the tendency to transition to the third limit, although without a clear turning in the trend. The observed behavior of turbulent flows represents an extension of the second limit behavior to higher pressures and temperatures. The influence of changing bulk strain rate on ignition temperatures was much smaller than the role of turbulence at all pressures.

The observed ignition trend can be explained by considering discrete mixing by turbulent eddies similar in size to the ignition kernel, which can bring together pockets of reactants, radicals, and high temperature gasses that would not otherwise mix. In the second limit, where ignition is governed by the fast reactions that define the crossover temperature, slower HO_2 reactions may be enhanced by the re-introduction of these radicals to the ignition kernel. This new source of chain branching would provide a boost to ignition. As the turbulence intensity, and thereby frequency, increases, the time available for this new branching pathway to operate decreases and the ignition temperatures increase somewhat. Similarly, at higher pressures where ignition is controlled by the slower HO_2 pathways, the reduced residence time due to turbulent fluctuations will hinder ignition such that turbulent ignition temperatures become higher than in laminar flows.

This work is reported in Publication No. 1.

1.3 Modeling study of turbulent nonpremixed ignition
The above experimental study on the effects of turbulence on nonpremixed hydrogen ignition showed that optimal conditions for ignition exist in weakly turbulent flows where the ignition temperature is lower than either laminar or strongly turbulent flows at the same pressure. In order to understand this phenomenon, computational simulation was conducted using Monte Carlo techniques to solve a joint scalar PDF equation. The simulation involved calculating the velocity field using a Reynolds stress model, and using this frozen flow field in the subsequent ignition calculation. The decoupling is justified because the small amount of heat release prior to ignition is not expected to affect the flow field. Results show that under most flow conditions, there is a large increase in H at ignition that is orders of magnitude larger than the background fluctuations. Heat release is shown to be negligible prior to ignition by examining the stochastic particle temperatures conditioned on the mixture fraction. After ignition has occurred, effects of heat release are evident in the conditional temperature data and the partially decoupled reactions are no longer expected to accurately represent the flow conditions.

Figure 3 shows that, at atmospheric pressure, the calculated ignition temperatures are about 30K higher than the calculated laminar ignition temperatures, and no appreciable variation is noted for flows with different turbulence intensities. Similar over-predictions were noted between turbulent and laminar calculations at pressures up to 3-4 atm. At still higher pressures, the turbulent calculations do not clearly exhibit the third limit behavior found in laminar ignition. These results differ from the experiment which did find an effect of turbulence intensity on ignition temperatures and show a decrease in ignition temperature with bulk strain rate instead of the increase shown in the turbulent calculations. At higher pressures, the quantitative agreement between turbulent calculations and experiments improved but it is unclear whether the trends of the two sets of data are qualitatively similar. Further modeling work is being conducted aiming to resolve this discrepancy.

This work is reported in Publication No. 2.

1.4 Nonpremixed ignition of H₂/air in a mixing layer with a vortex

To provide further insight into turbulent ignition in general and optimize ignition in particular, nonpremixed ignition in an elemental structure of turbulent flows, namely the vortex, was computationally investigated for hydrogen/air in a mixing layer, with the fuel side being pure hydrogen at 300K, and the oxidize side being hot air at 2000K.

Figure 4 shows the maximum heat release rate for mixing layers with and without (1D) the vortex. It is seen that, compared to the 1D case, the vortex case has higher heat release rates and an additional peak, hence signifying the presence of two-staged ignition. The first ignition occurs in a diffusion mode with chain branching reactions dominating. The second ignition takes place in the premixed mode, with more chemical reactions involved, and is substantially affected by the heat and species generated in the first ignition event. Results further show that the scalar dissipation rate is a crucial controlling factor for ignition, which causes a nonmonotonic dependence of ignition delay on all the vortex parameters.

This work is reported in Publication No. 3.

2. Chemical Kinetics of Laminar Counterflow Ignition

2.1 Premixed hydrogen/air and propane/air ignition

Nonpremixed ignition of H_2/Air has been extensively studied in previous years, yielding results that can be largely interpreted on the basis of homogeneous systems. While these results are fundamentally interesting and technically important, there exist many practical situations in which the ignition of a premixture is of relevance. Examples include the initiation of accidental explosions of a premixed combustible and ignition in the mixing layer of the hot re-circulation zone for flame holding. Furthermore, within turbulent flames there are pockets of unburned combustibles that could be ignited by the hot combustion products. Since the structure and response of nonpremixed and premixed flames are qualitatively different, it is therefore of interest to extend our studies on nonpremixed ignition to premixed ignition.

The problem studied is that of the ignition of a premixed hydrogen/air jet by a heated counterflowing inert jet. Figure 5 shows that the ignition temperatures decrease when the mixture equivalence ratio (ϕ) is reduced from 0.5 to 0.2. This is surprising since the mixture reactivity is expected to be higher, and the ignition temperature lower, as ϕ approaches unity for the present lean mixtures. This interesting behavior can be explained by realizing that the global ϕ, evaluated at the cold boundary, does not directly indicate the mixture stoichiometry in the ignition kernel, and hence is not the appropriate parameter to represent the system stoichiometry. The ignition kernel is located on the hot side of the flow and is formed by the diffusion of fuel and oxidizer from the reactant side. The large diffusivity difference between H_2 and O_2 causes the more diffusive H_2 being relatively enriched as the mixture diffuses towards the hot flow. As a result, the ignition kernel is much richer than the initial reactant mixture. When the boundary ϕ becomes leaner, the local ϕ in the kernel moves towards stoichiometric, the mixture reactivity increases, and the ignition temperature decreases.

One of the consequences of the existence of the oxygen-deprived kernel is that reaction rates decrease to the point where diffusive transport of the H atom from the kernel becomes important. The diffusive loss is most pronounced on the hot side of the kernel because the increasingly rich mixture reduces reaction rates further, resulting in a tail to the H concentration profile towards the hot boundary. In contrast to nonpremixed ignition, the diffusive transport is similar in magnitude to the chain terminating reactions, so premixed ignition temperatures are typically 80K higher than nonpremixed ignition temperatures and are more sensitive to changes in the strain rate.

The dearth of oxidizer in the ignition kernel can be remedied by adding small amounts of oxygen to the hot nitrogen flow. It was found that the ignition temperatures approach nonpremixed values by adding as little as 1% O_2 to N_2, while further oxygen addition has little effect as shown in Fig. 6. Thus by increasing the reaction rates and reducing the diffusive loss, the stoichiometry of the premixed kernel with oxygen addition becomes similar to that of the nonpremixed kernel even though the total amount of oxidizer is different. This therefore constitutes the transition between premixed and nonpremixed ignition. In practical situations, it is reasonable to expect that some amount of the oxidizing species would be present in the hot flow, perhaps as a result of lean combustion or the dissociation of combustion products, and the scenario of premixed ignition with oxidizer doping is a possibility that needs to be considered.

This study was further extended in two directions: hydrogen ignition at elevated pressures, and propane ignition at atmospheric pressure.

The study on hydrogen/air ignition at elevated pressures was motivated by the recognition that ignition phenomena are inherently sensitive to detailed chemistry, and that such sensitivity is strongly manifested in terms of pressure variations. Figure 7 compares the characteristic Z-shaped pressure-temperature explosion limits of a homogeneous mixture with the present premixed counterflow ignition temperatures, determined from both experiment and calculations, for 9% H_2 in air mixture ($\phi = 0.236$) versus heated N_2 at a pressure-weighted strain rate of k = $216s^{-1}$. The results show two important distinctions between the homogeneous and the present premixed ignition situations. First, the counterflow ignition response curve is shifted along the crossover temperature path to a higher temperature regime due to the reduced residence time. Second, the ignition temperature exhibits five limits over the pressure range investigated. These five ignition limits have the following characteristics.

The first three ignition limits qualitatively mimic the homogenous case. Quantitatively, the pronounced H radical loss to the hot inert side pushes the first limit to end at a higher pressure. The steepening of the second limit, which turns and forms the third limit, is due to the increasing importance of R-18 ($HO_2 + H_2 \rightarrow H_2O_2 + H$). This reaction converts the relatively inert HO_2 to the more reactive H radical and is greatly facilitated by the abundant H_2 within the ignition kernel owing to its preferential diffusion over O_2. As the concentration of H is built up with pressure, reactions between HO_2 and H (R10: $HO_2 + H \rightarrow H_2 + O_2$ and R11: $HO_2 + H \rightarrow OH + OH$) start to influence ignition. The combined effect is to weaken the termination reaction R9 ($H+O_2+M \rightarrow HO_2+M$) by a factor of $2k10/(k10+k11)$. Ignition occurs at a lower temperature than the crossover temperature, and an extended second limit behavior appears. Finally, as more HO_2 are produced with increasing pressure, its recombination reaction R14 ($HO_2 + HO_2 \rightarrow H_2O_2 + O_2$) generates H_2O_2 which further decomposes to

two OH through R16 ($H_2O_2 + M \rightarrow 2OH + M$). Thus ignition again becomes easier at the fifth limit. As a whole, the five limits of premixed ignition can be interpreted as a global three limits behavior, with the third (explosion) limit interrupted by the extended second limit which is the observed fourth ignition limit.

The counterpart of hydrogen/air ignition is propane/air ignition because propane, being less mobile than oxygen, will render an originally lean mixture more fuel lean in the ignition kernel. Thus while increasing ϕ will facilitate ignition, the extent is expected to be weakened. Figure 8 shows that the ignition temperature decreases with increasing ϕ, although the influence of preferential diffusion cannot be readily separated out.

This work is reported in Publication Nos. 4 and 5.

2.2 Counterflow ignition temperatures and laminar flame speeds of C_2-C_3 hydrocarbons at atmospheric and elevated pressures

While extensive kinetics data exist for hydrogen and methane, comparatively fewer data have been acquired for the hierarchically more complex C_2 and C_3 hydrocarbons, which are important fuels and intermediate constituents in hydrocarbon combustion. Therefore, the primary objective of the present study is to acquire additional data on the nonpremixed counterflow ignition temperatures as well as the laminar flame speeds of most of the C_2-C_3 hydrocarbons, namely acetylene (C_2H_2), ethylene (C_2H_4), ethane (C_2H_6), propylene (C_3H_6) and propane (C_3H_8). These data cover the regimes of high-temperature oxidation in flames and low- to intermediate-temperature oxidation relevant for ignition, in premixed as well as nonpremixed situations, and with substantial pressure variations. These data were then compared with those calculated by using an optimized mechanism for C_1-C_3 (Z.W. Qin, V.V. Lissianski, H.X. Yang, W.C. Gardiner, S.G. Davis and H. Wang, Proc. Combust. Inst. 28, 1663-1669, 2000) and an ethylene ignition mechanism (B. Varatharajan and F.A. Williams, J Propul. Power 18, 344–351, 2002). These two mechanisms are referred to as the Q- and VW-mechanisms respectively.

Results (Figs. 9 and 10) show that, for all ignition cases, the Q-mechanism consistently predicts higher ignition temperatures than the experiments, while the VW-mechanism agrees well with the experiments. On the other hand, the Q-mechanism agrees with the laminar flame speed data moderately well. For acetylene and ethylene, the Q-mechanism slightly over-predicts and under-predicts the lean and rich mixtures, respectively, as shown in Fig. 11 and 12. A possible source for the stronger reactivity of the Q-mechanism is that it was optimized against previous ethylene flame speed data based on linearly extrapolation, which yields higher laminar flame speeds. A fairly detailed exploration was conducted on the causes for the various disagreements between experiment and calculations.

This work is reported in Publication No. 6.

2.3 Ignition of dimethyl ether in counterflow

Dimethyl Ether (DME), CH_3OCH_3, is an attractive alternate fuel and fuel additive for diesel engines. The combination of its high cetane number and low boiling point of -25°C facilitates mixing, ignition, and cold start. The pyrolysis and oxidation process of DME have been studied mainly based on homogeneous systems, which has led to the development of two detailed mechanisms reported respectively in 1998 and 2003. However, their validity has not been experimentally scrutinized in nonhomogeneous

systems, particularly at low temperatures relevant for ignition. In the present study the ignition temperatures of DME in nonpremixed counterflow were experimentally measured and subsequently used to evaluate the accuracy of these two mechanisms.

Specifically, the ignition temperatures of nitrogen-diluted DME by heated air in counterflow were experimentally determined for DME concentration from 5.9 to 30%, system pressure from 1.5 to 3.0 atmospheres, and pressure-weighted strain rate from 110 to $170s^{-1}$. Figure 13 shows representative results for the ignition temperature as a function of DME mole fraction in nitrogen at 3atm and a pressure-weighted strain rate of $150s^{-1}$. It is seen that the ignition temperature monotonically decreases with increasing fuel concentration in the fuel jet, and that such a dependence becomes stronger for lower fuel concentrations. Furthermore, while the 1998-mechanism substantially over-predicts the ignition temperature, the 2003-mechanism agrees very closely with the experimental data. This observation holds for all results obtained in the present study.

Sensitivity analysis was performed to identify the differences between these two mechanisms. Overall, the 1998-mechanism shows much reduced sensitivity to the low temperature oxidation sub-mechanism, while the 2003-mechanism shows that the majority of the sensitivity comes from the low-temperature kinetics. For example, the 2003-mechanism exhibits a much stronger reactivity around 600K, as manifested by the turning point behavior (Fig. 14). On the contrary, the 1998-mechanism indicates the CH_3 radical concentration grows with the hot boundary temperature only gradually, which produces considerably less low temperature reactivity and therefore causes the ignition temperature to be 1039 K, which is about 100 K higher than that predicted by the 2003-mechanism. The reason that the low temperature kinetics contributes so much to ignition is that before the fuel enters the high-temperature ignition region around the hot-stream boundary, it is progressively heated from its low-temperature region.

The 2003-mechanism, consisting of 79 species and 398 elementary reactions, was then systematically simplified by using directed relation graph theory to a skeletal mechanism of 49 species and 251 elementary reactions, which in turn was further simplified by using computational singular perturbation and quasi-steady-state species assumption to a reduced mechanism consisting of 33 species and 28 lumped reactions. It was demonstrated that both the skeletal and reduced mechanisms mimic the performance of the detailed mechanism with high accuracy, as shown in Fig. 15.

This work is reported in Publication No. 7.

Publications

(a) Papers published in peer-reviewed journals

[1] "Effects of turbulence on nonpremixed ignition in heated counterflow," by J.D. Blouch and C.K. Law, *Combustion and Flame*, Vol. 132, pp. 512-522 (2003).

[2] "A joint scalar PDF study of nonpremixed hydrogen ignition," by J.D. Blouch, J.Y. Chen and C.K. Law, *Combustion and Flame*, Vol. 135, pp. 209-225 (2003).

[3] "Nonpremixed ignition of H_2/Air in a mixing layer with a vortex," by X. L. Zheng, J. Yuan, and C. K. Law, *Proceedings of the Combustion Institute,* Vol. 30, in press.

[4] "Ignition of premixed hydrogen/Air in heated counterflow," by X.L. Zheng, J.D. Blouch, D.L. Zhu, T.G. Kreutz and C.K. Law, *Proceedings of the Combustion Institute,* Vol. 29, pp. 1637-1644 (2003).

[5] "Ignition of premixed hydrogen/air by heated counterflow under reduced and elevated pressures," by X.L. Zheng and C.K. Law, *Combustion and Flame*, Vol. 136, pp. 168-179 (2004).

[6] "Experimental determination of counterflow ignition temperatures and laminar flame speeds of C_2-C_3 hydrocarbons at atmospheric and elevated pressures," by G. Jomaas, X. L. Zheng, D. L. Zhu, and C. K. Law, *Proceedings of the Combustion Institute,* Vol. 30, in press.

[7] "Experimental and computational study of nonpremixed ignition of dimethyl ether in counterflow," by X. L. Zheng, T. F. Lu, C.K. Law, C. K. Westbrook and H. J. Curran, *Proceedings of the Combustion Institute,* Vol. 30/1, pp. 1101-1109, (2004).

[8] "Development of comprehensive detailed and reduced reaction mechanisms for combustion modeling," by C.K. Law, C.J. Sung, H. Wang and T. F. Lu, *AIAA Journal*, Vol.41, No. 9, pp. 1629-1646 (2003).

Participating Scientific Personnel

1. C. K. Law, Principal Investigator

2. T. G. Kreutz, Research Staff

3. D. L. Zhu, Technical Staff

4. J. Y. Chen, Collaborator (UC-Berkeley)

5. J. D. Blouch, Graduate Student (Ph. D. awarded 2002)

6. G. Jomaas, Collaborating Graduate Student

7. T. F. Lu, Collaborating Graduate Student

8. X. L. Zheng, Graduate Student

9. J. Yuan, Collaborating Student

Biographical Data of Principal Investigator

Chung K. Law received a B.Sc. in Physics from the University of Alberta in 1968, an M.A.Sc. in Aerospace Studies from the University of Toronto in 1970, and a Ph.D. in Engineering Physics from the University of California in San Diego in 1973. After his formal education, he has been associated with the General Motors Research Laboratories as an Associate Senior Research Engineer from 1973 to 1975, with Princeton University as a member of the Professional Research Staff from 1975 to 1976, with Northwestern University as an Associate Professor and then Professor from 1976 to 1984, and with the University of California at Davis as a Professor from 1984 to 1988. He returned to Princeton University in 1988 and has been the Robert H. Goddard Professor of Mechanical and Aerospace Engineering since 1995.

Professor Law's research and teaching interests have included droplet and spray combustion, flame structure studies, aerodynamics and chemical kinetics of flames, ignition and extinction phenomena, pollutant generation and control, formulation and utilization of alternate and high-energy fuels, combustion instability, metals combustion, catalytic combustion, microgravity combustion, waste incineration, and combustion synthesis of materials. He received the 1984 Curtis W. McGraw Award of the ASEE, a Silver Medal from the Combustion Institute in 1990, the 1994 Propellants and Combustion Award, the 1999 Energy Systems Award, and the 2004 Pendray Literature Award of the AIAA, and the 1997 Heat Transfer Memorial Award of the ASME. He is a Fellow of the AIAA and ASME, a past president of the Combustion Institute, and a member of the National Academy of Engineering. He is author or co-author of over 300 archival publications in combustion, propulsion, and heat and mass transfer.
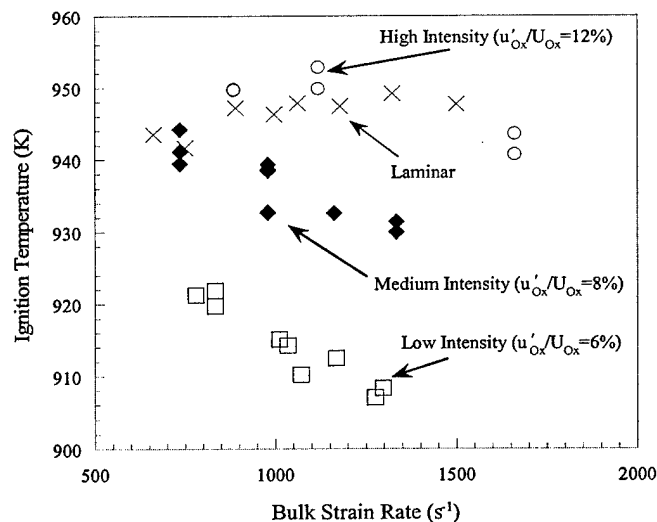
Figure 1: Effect of turbulence intensity on ignition temperature at 1atm and 20% H_2 concentration.
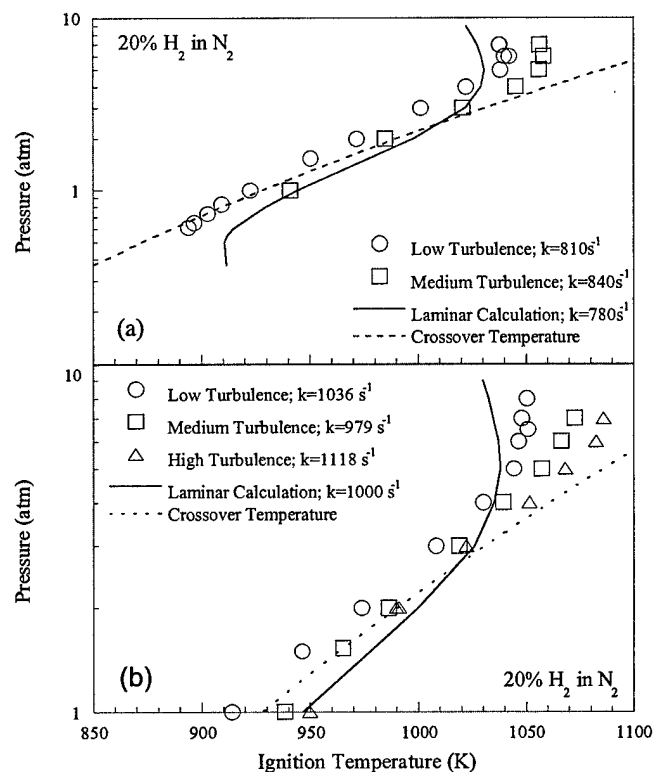
Figure 2: Effect of pressure on ignition temperature for different turbulence intensities.
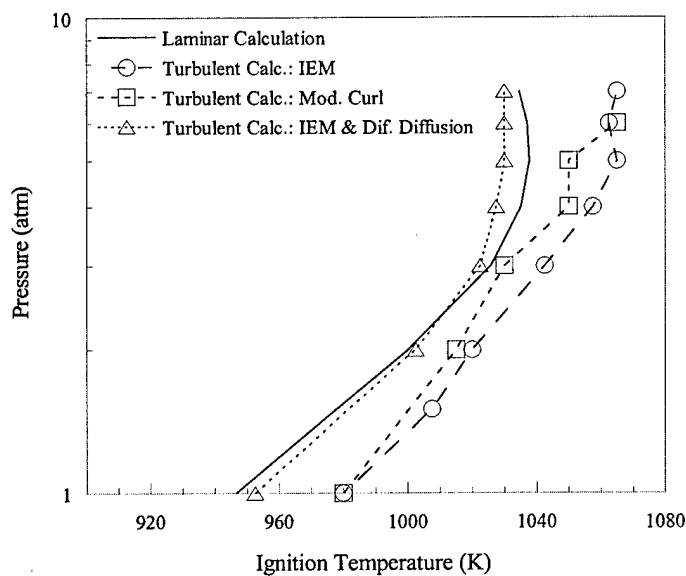
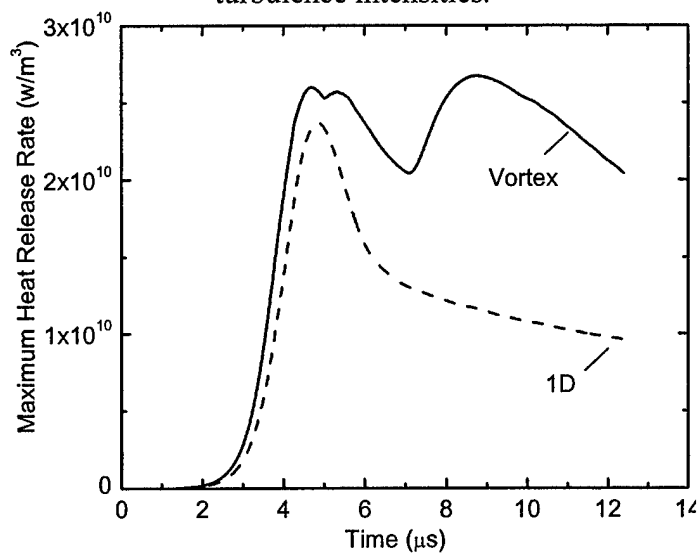Figure 3: Comparison of the effects of different mixing models on the ignition response to changing pressure.

Figure 4: Effect of turbulence intensity on ignition temperature at 1atm and 20% H_2 concentration.
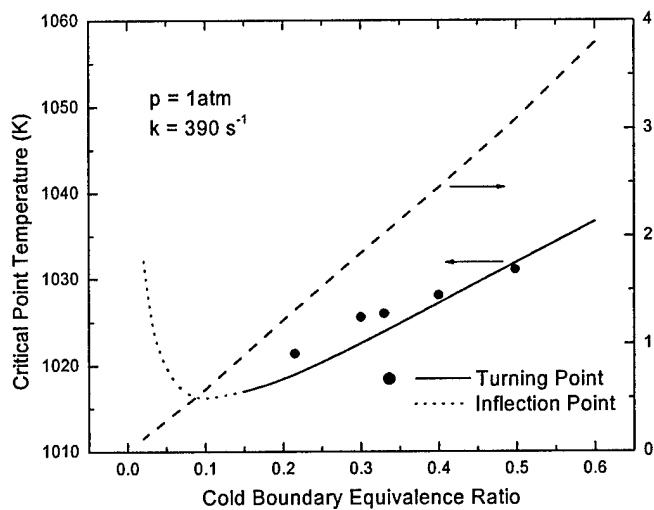
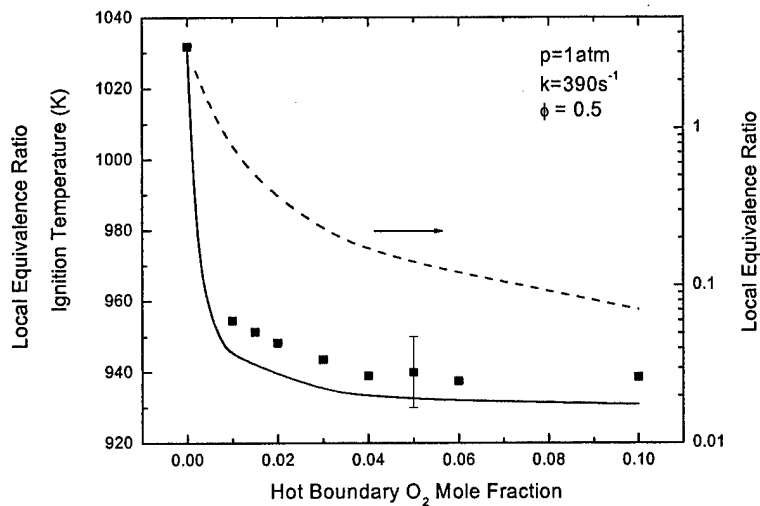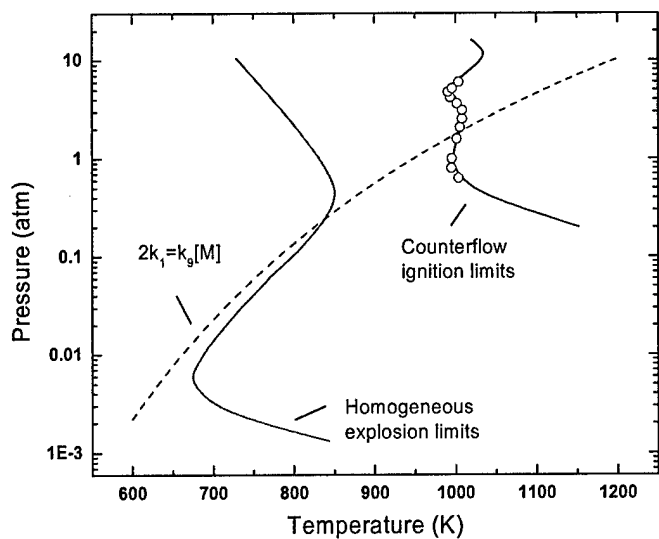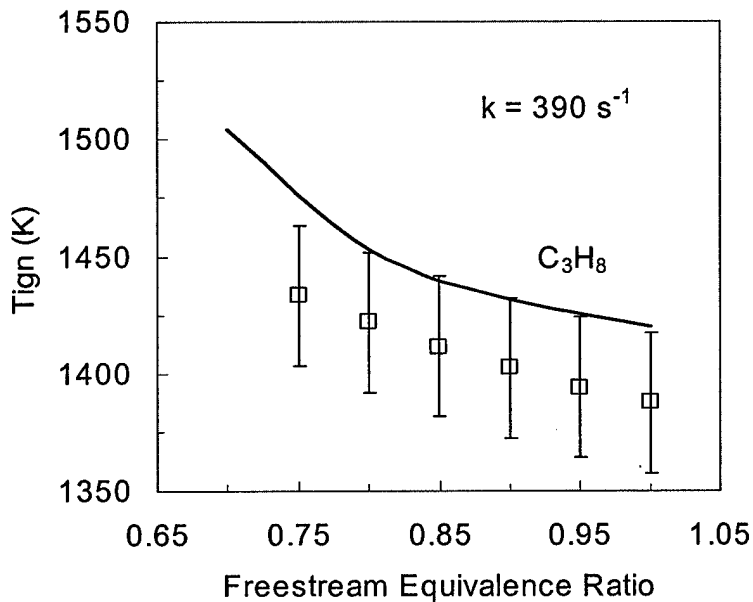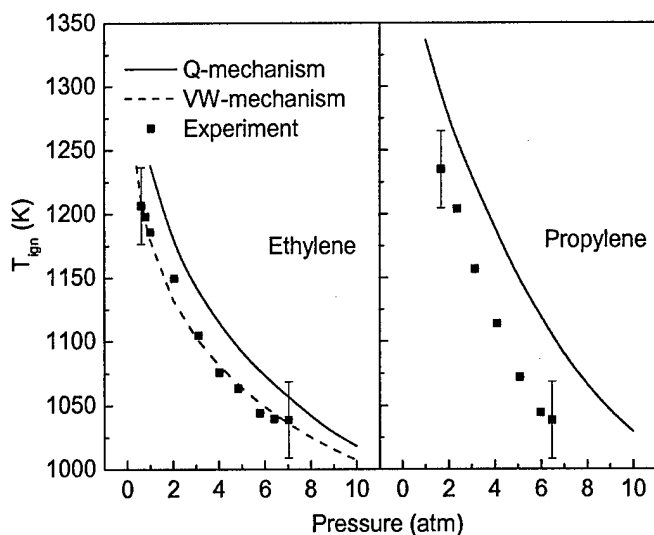Figure 5: Critical temperatures and local ϕ as functions of boundary ϕ.

Figure 6: Effect of adding O_2 to the hot side on the ignition temperature.

Figure 7: Comparison of the effects of different mixing models on the ignition response to changing pressure.

Figure 8: Effect of turbulence intensity on ignition temperature at 1atm and 20% H_2 concentration.

Figure 9: Effect of pressure on ignition
temperatures for C_2H_4 and
C_3H_6. Conditions: 5.9% Fuel in
N_2 and k=150s^{-1}
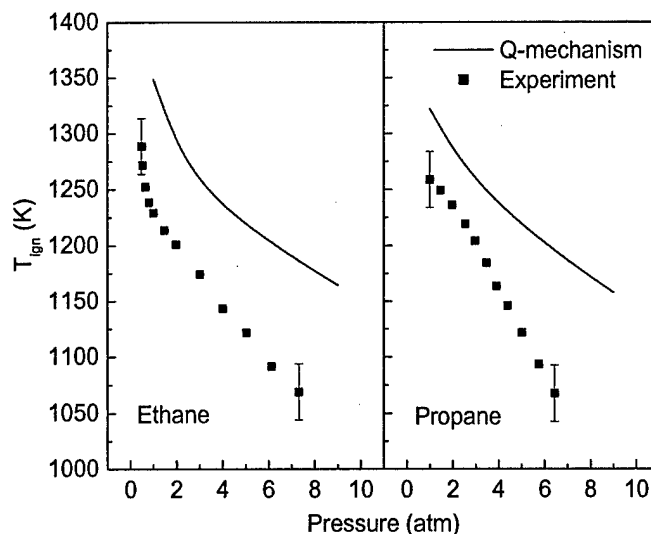
Figure 10: Effect of pressure on ignition
temperatures for C2H6 and
C3H8. Conditions: 5.9% Fuel
in N2 and k=150s-1
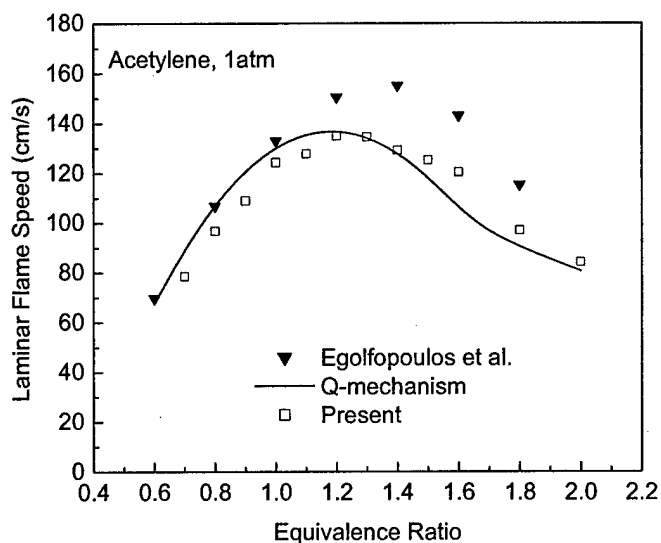
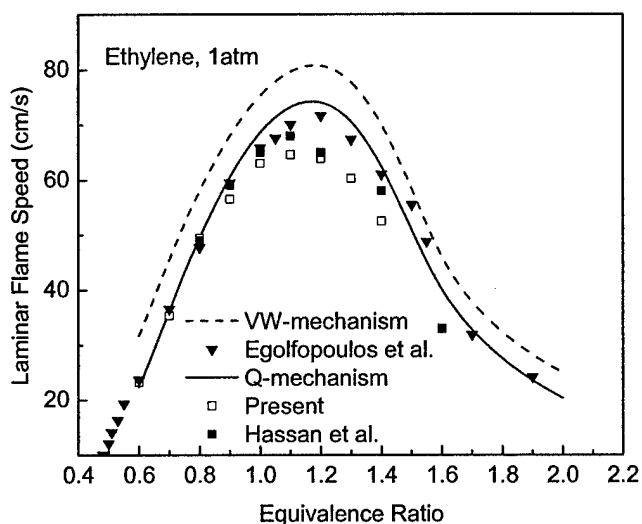Figure 11: Laminar flame speed of
acetylene (C_2H_2) in air at 1atm

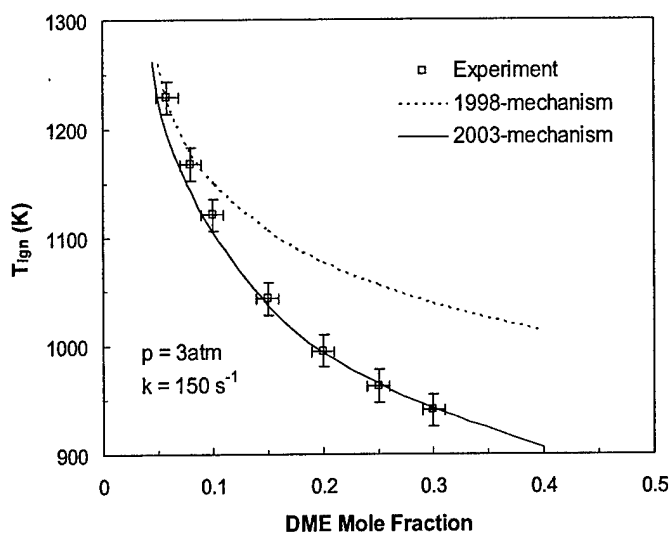Figure 12: Laminar flame speed of
ethylene (C_2H_4) in air at 1atm.

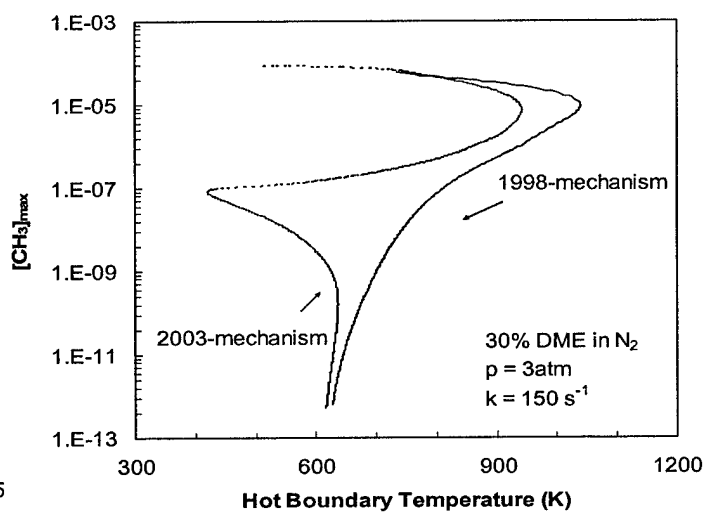Figure 13: Effects of DME mole fraction on ignition temperature.

Figure 14: Calculated S-curves for 30% DME in N_2 mixture with 150 s^{-1} strain rate at 3atm, using both mechanisms
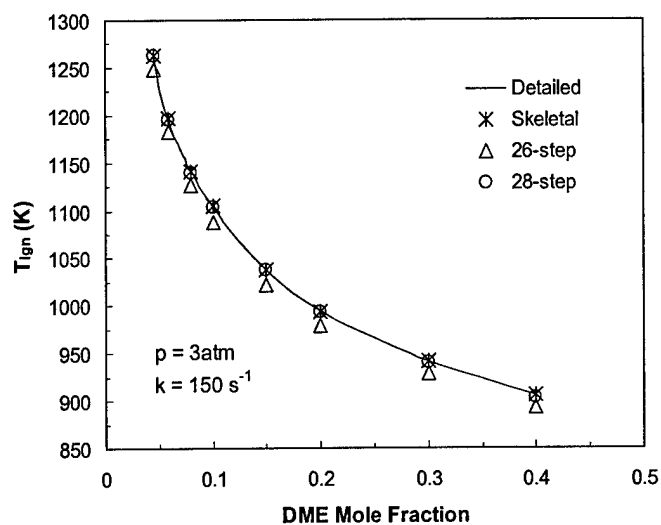

Figure 15: Comparison of the computed results using detailed, skeletal and reduced mechanisms for the ignition temperatures.